Cryogenic system for interferometric measurement of dimensional changes at 40 K: Design and performance

Peter Blake[*a], Franklin Miller [a], Tim Zukowski [b]
Edgar R. Canavan [a], Allen Crane [c], Tim Madison [a], David Miller [d]
[a] Goddard Space Flight Center, Code 551, Greenbelt, MD 20771
[b] Research Support Instruments, Lanham MD; [c] ATK, Inc., Beltsville, MD
[d] Bastion Technologies, Inc, Houston TX

ABSTRACT

This report describes the facility, experimental methods, characterizations, and uncertainty analysis of the Cryo-Distortion Measurement Facility (CDMF) at the Goddard Space Flight Center (GSFC). This facility is designed to measure thermal distortions of structural elements as the temperature is lowered from 320K to below 40 K over multiple cycles, and is capable of unattended running and data logging. The first measurement is the change in length and any bending of composite tubes with Invar end-fittings. The CDMF includes a chamber that is efficiently cooled with two cryo-coolers (one single-stage and one two-stage) rather than with liquid cryogens. Five optical ports incorporate sapphire radiation shields – transparent to the interferometer – on each of two shrouds and a fused silica vacuum-port window. The change in length of composite tubes is monitored continuously with displacement-measuring interferometers; and the rotations, bending, and twisting are measured intermittently with theodolites and a surface-figure interferometer. Nickel-coated invar mirrors and attachment mechanisms were developed and qualified by test in the CDMF. The uncertainty in measurement of length change of 0.4 m tubes is currently estimated at 0.9 micrometers.

Keywords: cryogenic, cryocooler, interferometry, dilatometer, ISIM, JWST, metrology, sapphire windows

1. INTRODUCTION

The James Webb Space Telescope Instrument Support Integration Module (ISIM) is being designed and developed at the Goddard Space Flight Center (GSFC). The ISIM Thermal Distortion Testing (ITDT) program was started with the primary objective of validating the ISIM mechanical design process – by demonstrating the ability to predict thermal distortion in composite structures at cryogenic temperatures using solid element models.

The first items to be tested were tubes designed with the same dimensions, laminate, and invar fittings as the proposed structure (Figure 1 ISIM composite tube). The distortions were to be measured in the transitions between 293 K and 40 K. The metrology requirements are listed in table 1.

Figure 1 ISIM composite tube, with Invar end plugs

[*] peter.n.blake@nasa.gov; phone 301 286-4211; fax 301 286-0204

Table 1. Tube metrology requirements

Tube length	404 mm
Tube cross-section	75 mm
Materials	Graphite/epoxy laminate 2 square plugs invar 36 Epoxy adhesive
Expected length change from 293K to 40K	~ 36 µm
Required uncertainty in measurement of length change	1.5 µm
Required uncertainty in measurement of bending and twist	6 sec

2. FACILITY DESIGN

The Cryo Distortion Measurement Facility (CDMF) was designed to meet the requirements of this first cryo-distortion test of ISIM tubes, and to be generally useful in anticipated future tests. The basic concept is that a cryochamber or dewar with several ports would enclose and control the temperature of the test articles, which would be populated with reflecting targets. Displacement-measuring interferometers (dmi's) would continuously record the change in displacement of the two ends, yielding the ΔL measurement; and theodolites or other position-sensing detectors would measure the rotations of attached targets. Part temperatures would be uniform during thermal transients so that thermal strain data could be taken continuously from 320K to 40K.

2.1 Cryochamber

A mechanically cooled cryo-chamber was chosen in preference over a liquid-cryogen dewar, since it could, in safety, be left running overnight under automated control. We have made continual improvements in the hardware and computer controls to allow unattended round-the-clock operation. Runs will be slower with a cryocooler, compared to the use of cryogens, with their enormous cooling capacity; but both labor and expended material costs will be much lower.

The inner test volume is 0.86 m x 0.58 m x 0.25 m, anchored by a cold plate, on which the test objects would rest, and to which they could be thermally strapped, if desired. Surrounding the cold plate would be two shrouds of increasing temperature, all enclosed by a vacuum enclosure, with windows of fused quartz.

The design of the chamber included two inner shrouds, thermally isolated, with the outermost of the two shrouds designed to cool to about 100K (actual achieved: 160K), and the inner shroud cooling to 20K (actual: 35K). Figure 2 and Figure 3 show the design of the cryochamber. The outer shroud would be thermally connected to the first stage of a two-stage cooler, and the inner shroud connected to the second stage. Later in the program, a second cooler was added to the cold plate for additional cooling power. The cold stage gets approximately 75 watts of cooling power at 100K from the single stage cooler and 22 Watts of cooling power at 100 K from the second stage of the two-stage cooler.

Another design criterion was low transmitted vibration to the test articles. This criterion might be more important in possible future measurements than in the current measurement, since as long as the dmi's maintain lock, vibration can be averaged out of the measurement stream. Design features included a soft connection between the thermal bus and the cold plate (Figure 4). Another design feature, a gas gap in the thermal linkage between the cryocooler and the thermal bus, was perhaps mishandled, leading to a disappointing thermal transfer from the outer shield, which is why the outer stage runs at 160K, rather than at 80K. This gas linkage had a second problematic effect: it prevents us from using a optical bench floated on air-bearings, since the motions of the table when pushed on by personnel (which is unavoidable) would crash the gas-gapped parts into each other. Consequently, the facility was not floated on the air bearings. Ordinary vibrations came through the floor into the table, but did not cause any problems (section 3).

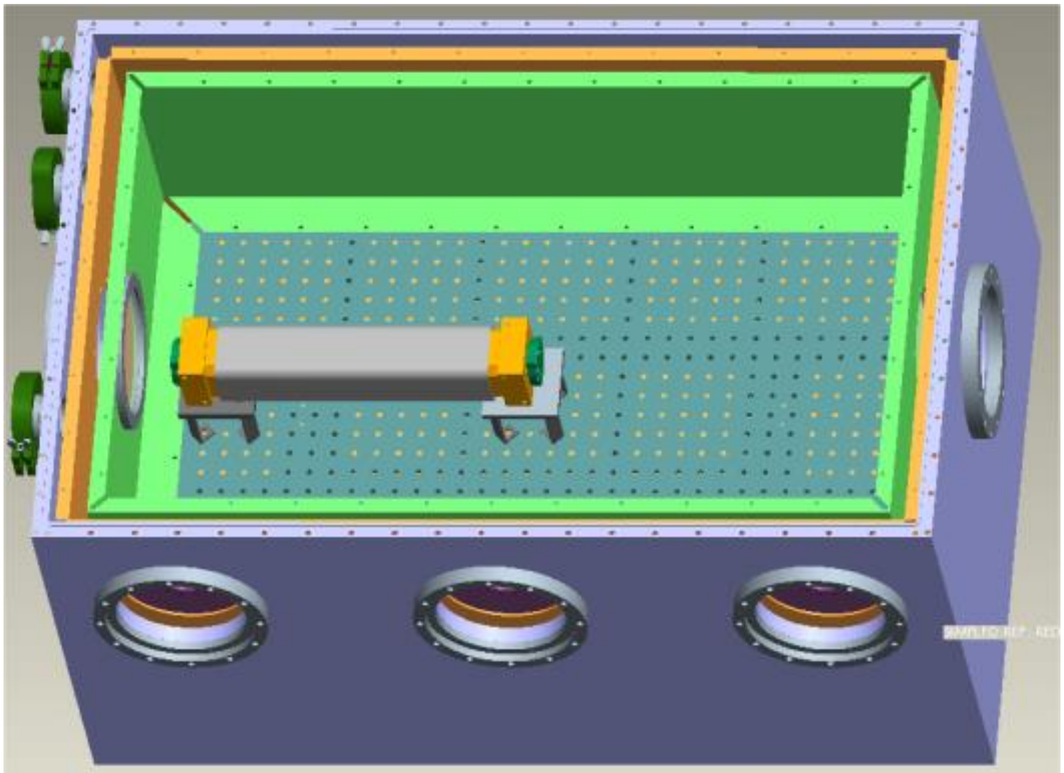

Figure 2. Isometric view of the CDMF cryochamber, showing a tube placed on the cold plate.

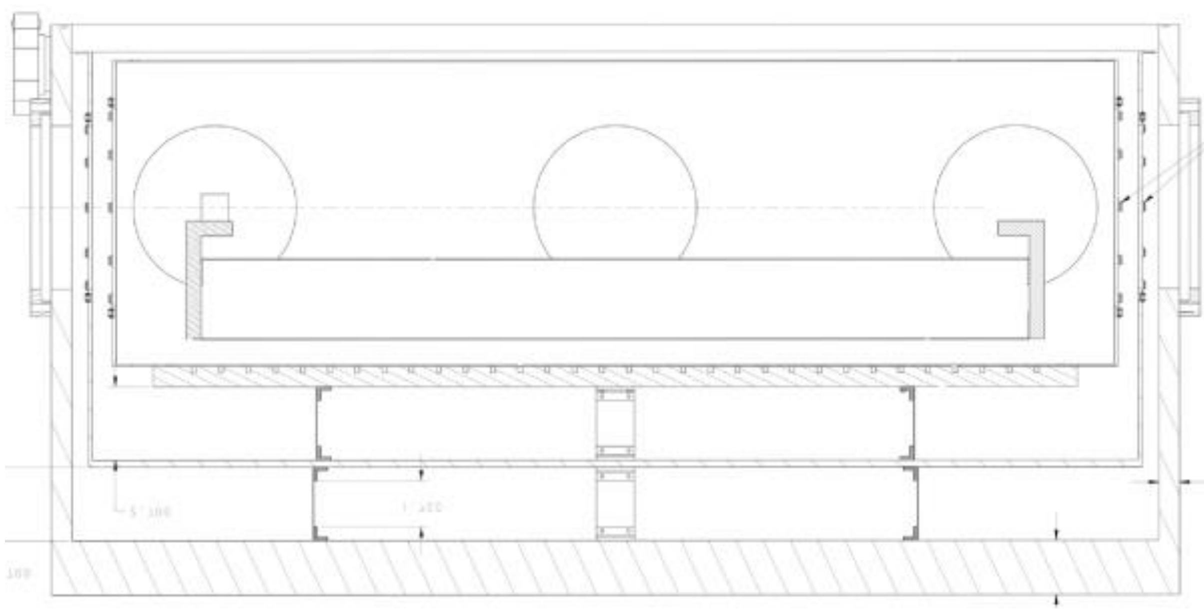

Figure 3. Side view of the cryo-chamber, showing the thick vacuum walls, the two thermal shrouds set off by insulating flexures, the cold plate with attached test article, and in the back walls, three metrology ports.

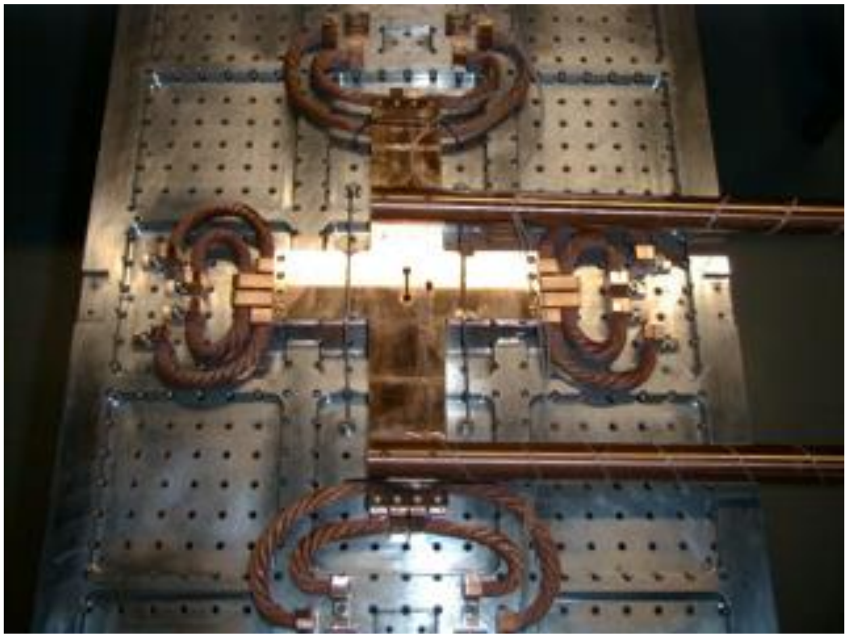

Figure 4 Connection of thermal bus to cold plate

2.1.1 Radiation shields

With these cooling rates several large openings, with views of the vacuum chamber port windows, would overwhelm the cooling with their thermal radiation. Possible solutions include stopping down the ports to the smallest possible apertures with sheet metal. Our choice was to fasten radiation shields: thermally conductive windows transparent to the wavelengths used in the metrologies. The material chosen would have to be amenable to the fabrication techniques of a standard optical shop, and capable of being fabricated to $\lambda/4$, with high transmission. The simplest solution would be to use glass or fused silica. A thermal model was run for a glass window as the radiation shield on the outer shroud, held at 76K (Figure 5). The center of this window would reach a temperature over 180K: which would be radiating consequent heat onto the inner shield at an unacceptable level.

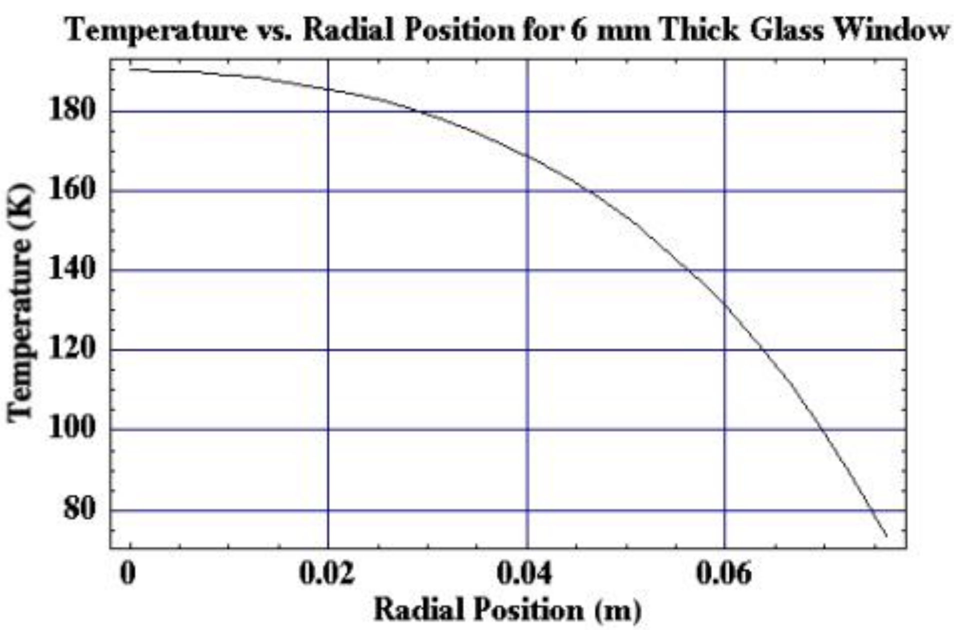

Figure 5.   Modeled temperature of glass radiation shield on outer thermal shroud

Clearly, a shield with higher thermal conductivity was desired. Suitable candidates included single-crystal sapphire, single-crystal quartz, and lithium fluoride. All of these materials have available a suitable anti-reflection (AR) coating that would allow Transmissions of over 98%. Since all interferometry requires control of polarization of the probing beam, the bi-refringence of the crystal must be minimized. Table 2 gives some properties of window materials:

Table 2. Radiation shield material properties

Material	Thermal conductivity at 100 K	Bi-refringence at 632 nm (Δn_i)	Apparent elastic limit	Flexure strength
Fused quartz	0.8 W/mK	0 if unstressed	55 MPa	110
Sapphire: cut perpendicular to the optic axis (c axis)	120 W/mK	-0.008 0 if cut perpendicular to c axis	300 MPa	1200
Single-crystal quartz: can also be cut to C-axis		+ 0.009 0 if c-axis		
Single-crystal LiF	90 W/mK	0: all axes (isotropic)	11 MPa	27

Although LiF has a lower birefringence, it is somewhat absorptive of water vapor and is said by suppliers to be very difficult to work, being soft and easy to damage. LiF is also sensitive to thermal shock. We chose single-crystal sapphire, with the plane perpendicular to the c-axis: 3 mm thick x 6” diameter.

2.1.2 Radiative v. conductive v. molecular cooling

Since cooling by radiative heat transfer scales as the fourth power of the temperature, the expected cooling of the test article by radiation is always expected to be low when the temperature of the cold plate and inner shroud fall below 100K. Two options were considered: 1) low pressure exchange gas (He) in the chamber to thermally couple the test article to the cold inner shield walls; and 2) thermal straps to conductively couple the invar plugs to the cold plate.

We used 1-D transient numerical models to calculate the temperature profiles in the test articles during cooldown for each option (Figure 6. Thermal gradient in test part in modeled cooldown.). The explanation of the large gradient under exchange gas is that our tubes have heavy metal end plugs with a relatively enormous heat capacity, compared to the thin-walled composite tubes. When cooled by radiation or exchange gas, the black carbon/epoxy tubes would cool down much faster than the heavy end plugs. We needed to use thermal strapping at both ends of the tube. Thermal straps connected the invar plugs to the cold plate.

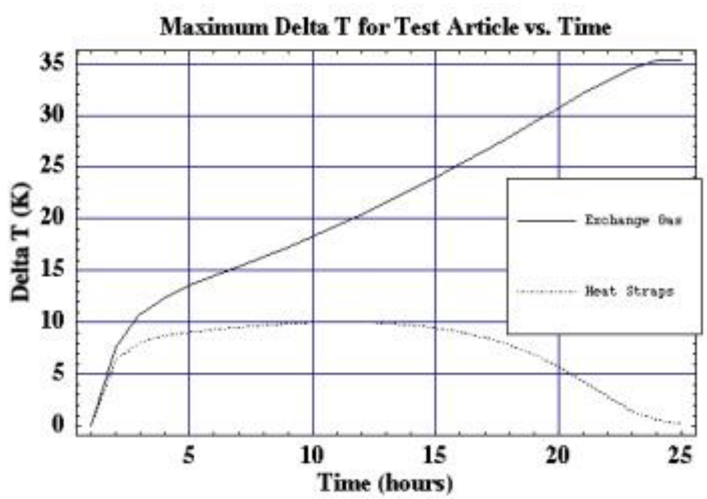

Figure 6. Thermal gradient in test part in modeled cooldown.

2.1.3 Stability

As will be discussed in section 3, the greatest source of uncertainty comes from the Abbe error created when the tube rotates in the plane of the cold plate (yaw). A strong effort was made to design the cold plate and the support of the test article such that rotations would be minimized. The two shrouds and the cold plate stack up on each other in a sequence starting at the vacuum chamber floor. Each step up was created by four symmetrically placed insulating flexures, placed such that the cold plate would stay centered in its own plane (Figure 3). Naturally, it would be expected to fall as the supports shrink with the lowering temperature, but the plate was designed to stay true with respect to rotations.

Since the test article is thermally strapped, there was also a requirement to mount it kinematically. A kinematic mount was designed for the tube. Two invar flexures, machined in one piece, were mounted to the aluminum cold plate (Figure 7). The top surfaces of the flexures were flat, and to them were bonded ceramic hemispheres and half-cylinders in such a pattern as to provide a kinematic positioning rest for three ceramic hemispheres bonded to the bottom surfaces of the invar end plugs (Figure 8).

The resultant success of the design in preventing rotations of the test article is given in the discussion on uncertainty.

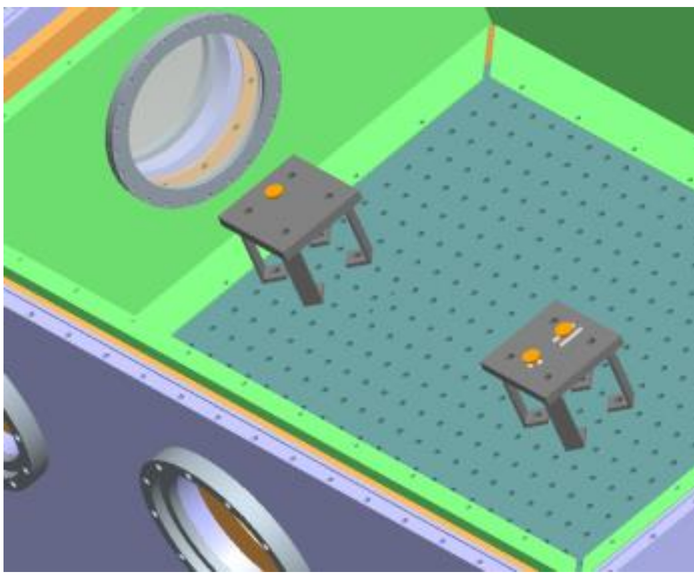

Figure 7 Invar flexures

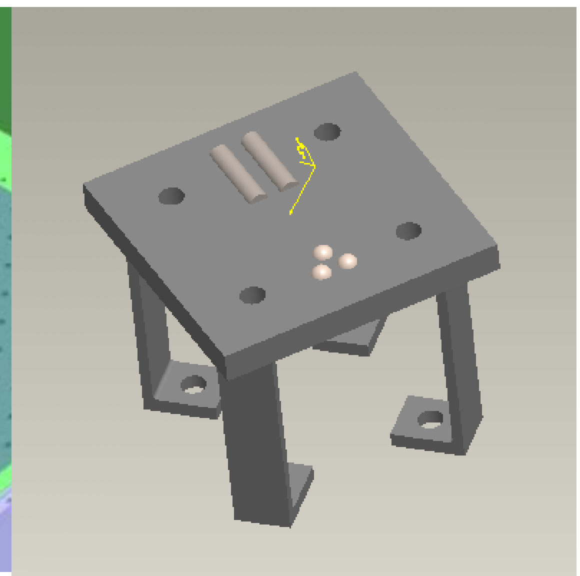

Figure 8 Kinematic positioning

2.2 Displacement-measuring interferometry

To measure the relative displacement of the two ends of the tube, heterodyne displacement measurement interferometry (dmi) was utilized, since heterodyne dmi is less sensitive to target tilt than pure Michelson interferometry. We used the Zygo ZMI 1000 system that we have had in the lab for many years. Two compact interferometers (model 2001), each measuring both displacement and one axis of tilt, were trained on flat mirrors fastened to each end of the tube. The interferometers were independently measuring displacement of each mirror from its start-up position; and the two displacements were subtracted to get the change in length.

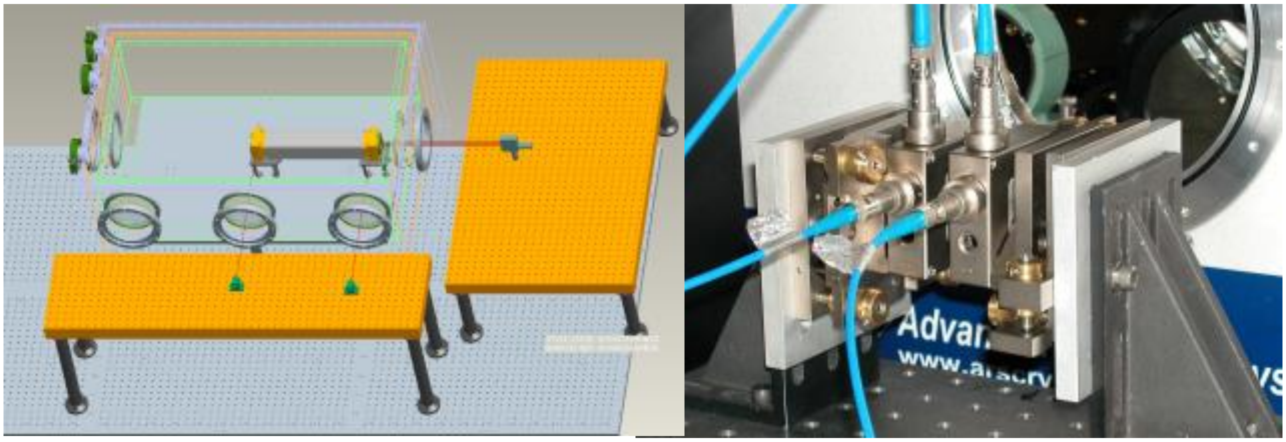

Figure 9 Support of compact dmi's

The Zygo compact interferometer[i] splits the incoming beam several times and sends four beams to the target (Figure 10). The displacement measured is the average displacement of the top two beams (*i.e.*, point A). In our set-up the four beams are arrayed vertically. The tilt between the points A and B is calculated in the computer system using the known value of the distance h (about 12.7 mm).

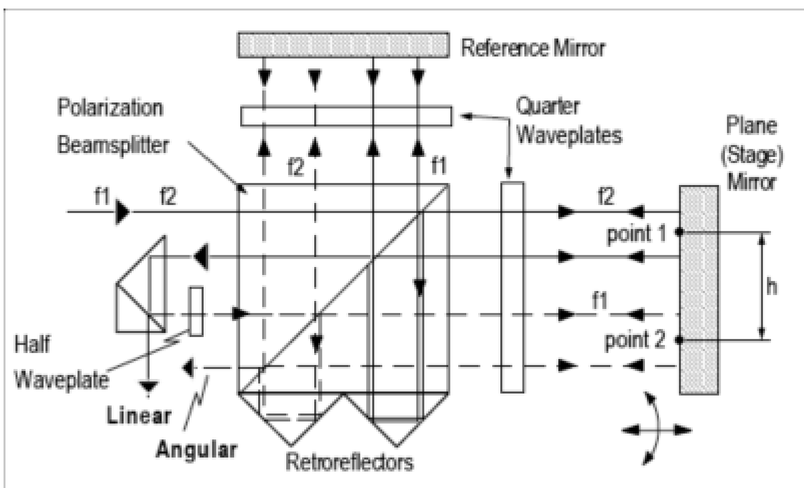

Figure 10 Diagram of compact interferometer

2.3 Targeting

Initially, we thought of using alignment cubes on the top surface of the plugs, and developed some invar alignment cubes, which worked quite well. But early modeling of the tubes indicated that at 40K, the composite tube, shrinking down, and squeezing the bonding tangs of the invar plug, would tilt the top surface of the plug backwards by 6 arcsec, which didn't seem like a lot until we realized, using simple geometry, that the measurement points midway in the two cube faces would be displaced towards each other from the center points of the tube faces by 2.5 µm each, giving an Abbe error of 5 µm. This illustrated for us the importance of keeping the measurement points as close to the central axis of the tube as possible.

The second targeting scheme was to use a flat mirror across the back of the tube, measured by a beam running down the center of the tube, passing through a hole in a flat mirror across the front plug face. The second interferometer would target the front "donut" mirror, placing its beam at a horizontal offset of 14.5 mm ± 0.3 mm.

The mirrors were made of invar, since our plan was to fasten through holes to the invar plugs. At first, the invar was polished in the optics shop, but the reflectance was only 35%; and with four reflections going round-trip through three windows, the power returning to the detector was too low. So now, both sides of each mirror needed to be polished and coated with protected aluminum. At this point we might have wished we had developed ULE or Zerodur mirrors for the test, but we pressed on with Invar.

The distortion of these mirrors at cryo is obviously a source of error that needed to be evaluated (Section 3).

The two compact interferometers in the CDMF are targeted on the front and back mirrors as illustrated in Figure 11.

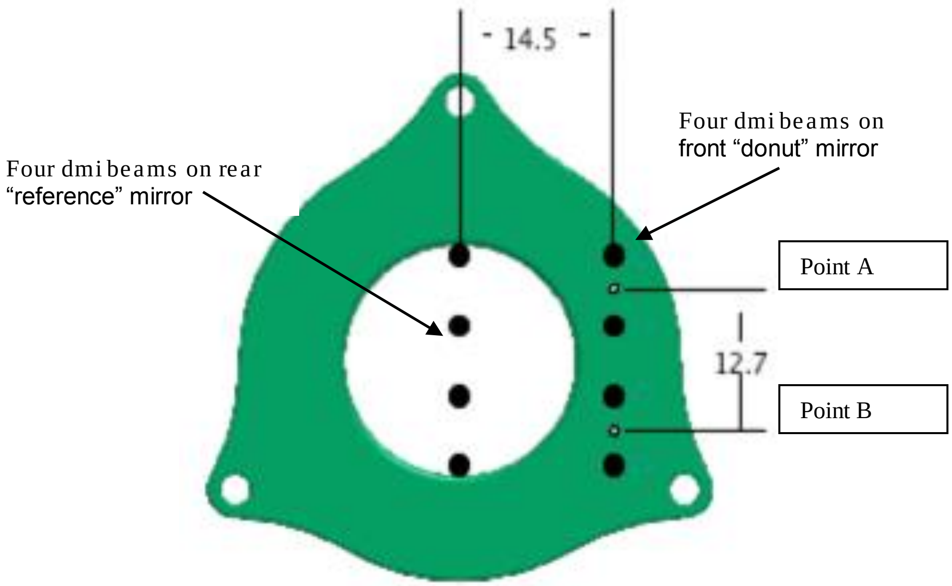

Figure 11 Beam locations of the two compact interferometers

2.4 Control

A control system, written in LabView, was developed for us. The system monitors temperatures, cooling system status, valve positions, interferometer readings, interferometer error signals, and other data. When an error is detected, the interferometer system is reset to zero, and the measurement continued, if possible. An automated phone call is sent out to the test personnel on call.

3. FACILITY CHARACTERIZATIONS

3.1 Temperature gradients

Temperature sensors with a 0.25K calibrated accuracy were used to insure that test assembly gradients did not exceed 1K laterally, and 4K axially. The temperature profiles during a single cycle are given in Figure 12. The axial gradient in the tube reached a maximum of 3 ½ K (Figure 13), while the lateral gradient remained below 1 K.

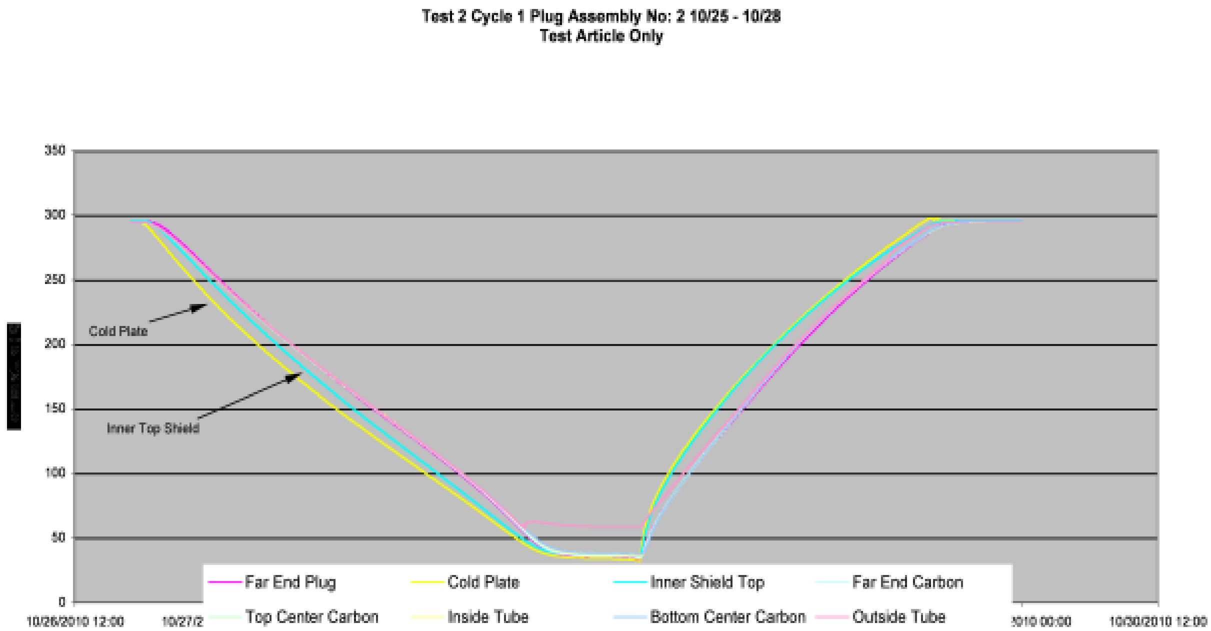

Figure 12. Temperature profiles during thermal cycle of ISIM tube in CDMF chamber

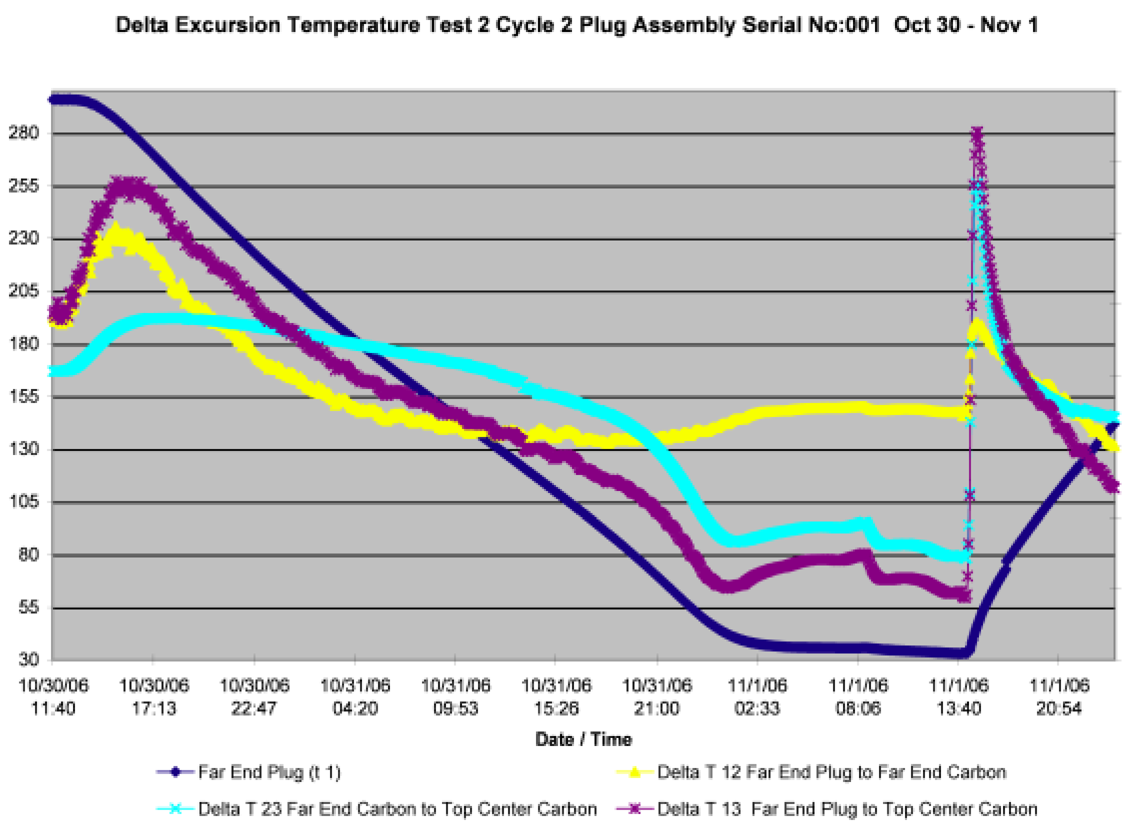

Figure 13 Temperature gradients in ISIM tube vs. time and cooldown temperature

3.2 Test article rotations and mirror distortions

The tops of the Invar flexures and the tops of Invar plug ends were populated with our Invar alignment cubes, secured with GE varnish. The test article tubes were placed in their kinematic supports, and trials were run from ambient to 36K.

Theodolites were used to measure angular motion values. The results are listed in Table 3 and are entered into the calculations of uncertainty given in Section 4.

Table 3 Motions of test article and targets from ambient to 40K

Rotation angles	Initial alignment uncertainty = 3 arcmin Horiz. rotation = 10 arcsec Vert. rotation = 20 arcsec
Nonparallel angle	e = 10 arcsec
Vertical displacement	dy = 400 μm
Beam parallel separation distance	Horiz. S = 14.5 mm Vert. S = 0.5 mm

The distortions of the two mirrors were measured with a figure-measuring interferometer. Because the table was not floated (section 2.1), we used an instantaneous phase-shifting interferometer. The results are given in Table 4.

Table 4 Target figure error

Target Figure Error	0.75 waves @ 632 nm

4. UNCERTAINTY CALCULATION

In measurement of the change in length of a 400 mm composite tube, based on the parameters given in section 3, the combined standard uncertainty[ii], u_c, is estimated to be 0.9 μm.

Six thermal cycles from 320K to 35K were conducted on two test assemblies (Figure 14). The standard deviation for the thermal strains between 293K and 40K for all transitions was less than 0.5 microns. This variation is contained within and accounted for by the variations described in section 4; but did not exhaust those variations. Therefore, it was determined that it did not need to be added to the combined standard uncertainty; nor could it be substituted for the combined standard uncertainty. Further analysis of the data will refine the estimate of uncertainty.

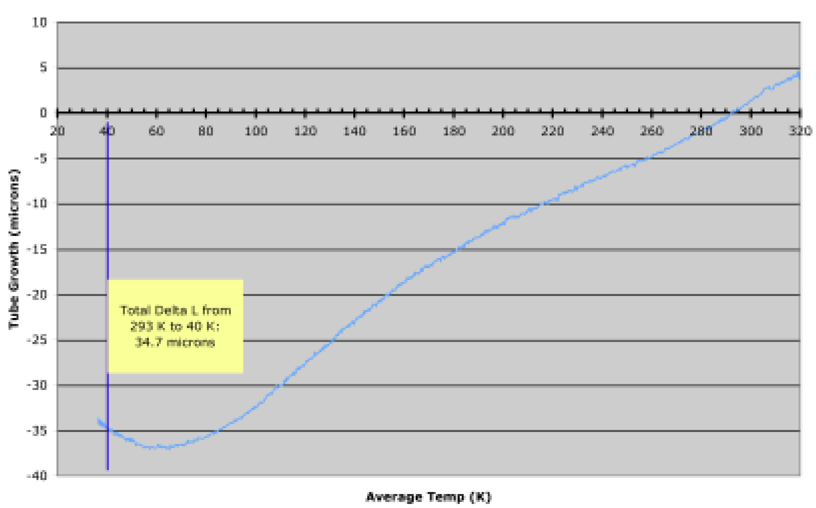

Figure 14 Sample run of CDMF: Delta L vs. temperature

Table 5 Uncertainty table.

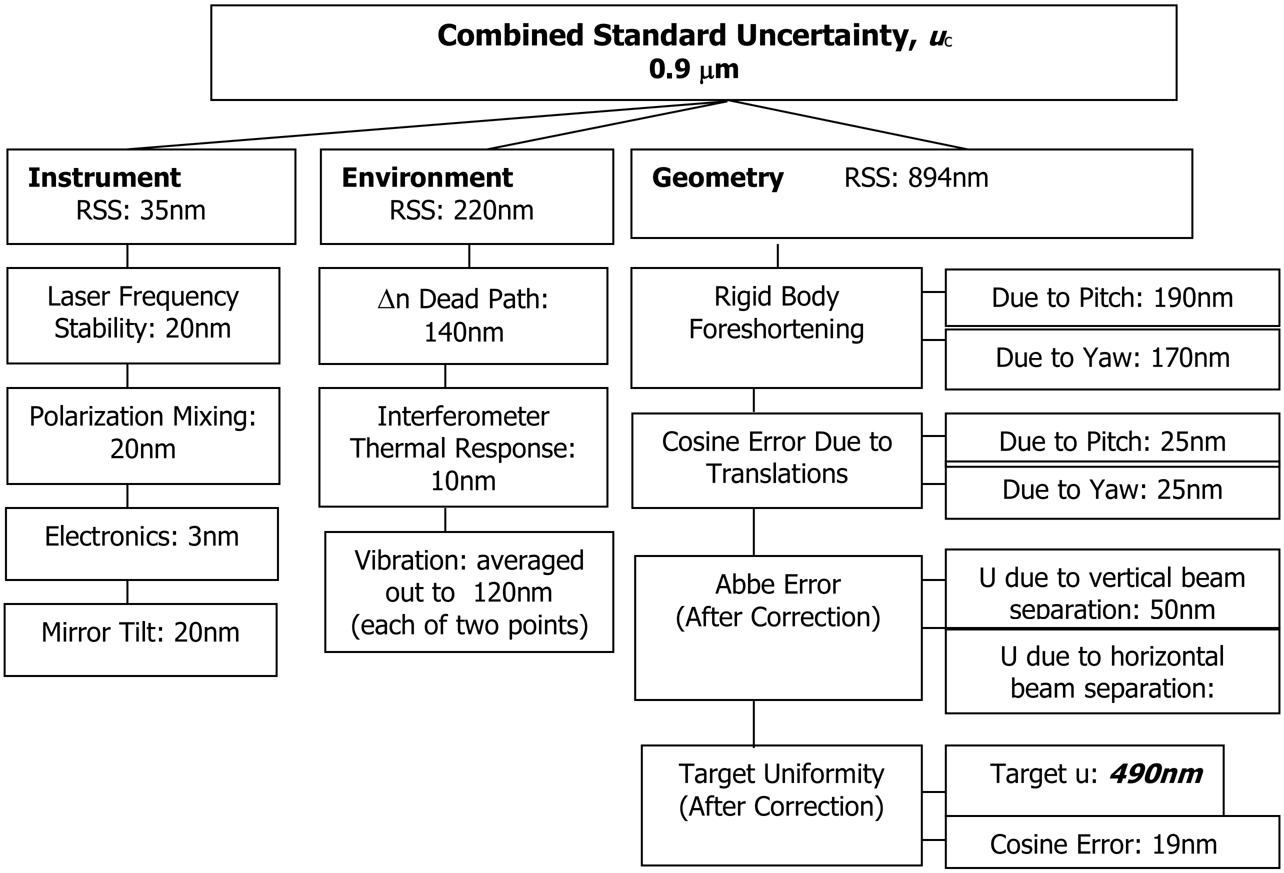

ACKNOWLEDGEMENTS

The authors gratefully acknowledge the assistance of the James Webb Space Telescope Project. Our thanks also to Advanced Research Systems (Macungie PA) for construction of the cryocooler, to Rayotech Scientific, Inc (San Diego) for the sapphire windows, to Betsy Rector of SGT(Beltsville MD) and Kareny Dominguez of Vigyan (Hampton VA) for their expert creation of control programs 1 and 2, and to Patrick Williams (SGT, Greenbelt MD), Barbara Zukowsi (Ball Aerospace, Lanham MD), and Dan Young (ATK, Beltsville MD) for their contributions to subsequent measurements. Thanks also to Colin Fletcher and Steven Mielke of Zygo Corp, Middlefield CT for their patient advice on the use of dmi's. Mention of trade names or commercial products does not constitute endorsement or recommendation by NASA.

REFERENCES

i Zygo Corp Manual, *ZMI Optics Guide*

ii B. Taylor, C.E. Kuyatt, "Guidelines for Evaluation and Expressing the Uncertainty of NIST Measurement Results", NIST Technical Note 1297, 1994